The transmembrane domain of diphtheria toxin improves molecular conjugate gene transfer

Krishna J. FISHER and James M. WILSON*

Institute for Human Gene Therapy and Department of Molecular and Cellular Engineering, University of Pennsylvania Health System, and The Wistar Institute, 3601 Spruce Street, Philadelphia, PA 19104-4268, U.S.A.

Vectors based on the formation of a soluble DNA–polycation complex are being developed for the treatment of human diseases. These complexes are rapidly taken up by receptor-mediated endocytosis, but are inefficiently delivered to the nucleus owing to entrapment in membrane-bound vesicles. In this study we introduced the transmembrane domain of diphtheria toxin into a DNA–polycation conjugate complex in an effort to increase gene transfer by membrane perturbation. The transmembrane domain of diphtheria toxin was expressed in *Escherichia coli* as a maltose-binding protein fusion and chemically coupled to high-molecular-mass poly-L-lysine. Incorporation of this conjugate into a traditional complex formed with a luciferase-containing plasmid with an asialo-orosomucoid–polycation conjugate significantly increased transfection efficiency *in vitro* in a manner proportional to the amount of diphtheria toxin incorporated. The delivery of luciferase RNA transcript was similarly increased when complexed with similar polycation conjugates. This study uses the structural biology of a bacterial protein to improve polycation-based gene delivery.

INTRODUCTION

Molecular conjugates composed of poly-L-lysine and plasmid DNA can be assembled to target specific cell types by receptor-mediated endocytosis. This method of gene transfer is easily adapted to deliver potentially therapeutic DNA species to diseased tissue, thereby forming the basis of a vector for gene therapy. The polycation carrier in these formulations serves two important functions: to condense the negatively charged nucleic acid into a soluble particle and to anchor receptor ligands and other ancillary factors. A variety of receptor ligands have been coupled to poly-L-lysine and tested for their ability to direct vector uptake, including galactose terminating sugars (which bind to the hepatic asialoglycoprotein receptor) [1], transferrin [2] and the Fab portion of polyclonal antibodies (e.g. to target the epithelial polymeric immunoglobulin receptor) [3].

Studies conducted *in vitro* and *in vivo* have demonstrated several parameters that can influence the efficiency of gene transfer mediated by a DNA–carrier complex. Early investigations into the physical properties of polylysine–DNA complexes indicated ordered polymer association was largely dependent on the salt concentration and the ratio of lysine to phosphate [4–6]. The length of polylysine was also shown to affect the size of polymer aggregates and the precipitation coefficient [6]. Most DNA–carrier complexes for gene transfer have been described as being approx. 100 nm in diameter forming a toroid-like structure, with each particle packaging multiple copies of plasmid DNA [2]. Perales et al. recently described a technique for generating particles 10 nm in diameter called 'unimolecular' structures, which were reported to have a substantially greater gene transfer efficiency *in vivo* when endocytosed via hepatic asialoglycoprotein receptors [7].

DNA–polylysine formulations internalized by receptor-mediated endocytosis are predominantly localized to membrane-bound vesicles shortly after uptake, and ultimately trafficked to lysosomes [8]. This represents a significant loss of delivered material and correlates with the low levels of gene transfer that are typically reported for DNA–polylysine complexes. Eukaryotic viruses and other pathogens that enter cells by receptor-mediated endocytosis encounter a similar barrier. To minimize lysosomal transport, these agents have evolved endosomolytic activity that perturbs the integrity of vesicle membranes, allowing the luminal contents to spill into the cytoplasm. This invariably involves pH-induced changes in the conformation or exposure of critical protein or lipid domains.

The membrane-disrupting activity of adenovirus and its effect on vesicle transport have been studied extensively. Within 30 min of binding to high-affinity receptors, most adenovirus particles are released from endosomes and shortly thereafter are found associated with the nuclear envelope [9]. Several reports have shown that impermeable macromolecules (e.g. fluorophores) that are co-internalized with adenovirus are similarly released into the cytoplasm with high efficiency [10–12]. It is now well documented that this phenomenon can be extended to soluble DNA–polylysine complexes. Substantial increases in gene transfer can be obtained by simply infecting cells with adenovirus in *trans* during transfection with complex [13]. However, the two particles can also be directly coupled, resulting in further improvements in gene transfer while minimizing cytopathic effects. This technique was introduced by Curiel et al. [14] and involved forming an antibody–antigen bridge between the DNA–polylysine complex and the adenovirus capsid. By reducing receptor uptake to a single-order event, the endosomolytic activity of adenovirus could be harnessed with a significantly

Abbreviations used: ASOR, asialo-orosomucoid; DT, diphtheria toxin; DTT, dithiothreitol; DTtm, 5′ end of DT cDNA (also transmembrane domain of DT); FBS, fetal bovine serum; HBS, Hepes-buffered saline; IPTG, isopropyl β-D-thiogalactoside; MBP, maltose-binding protein; sulpho-LC-SPDP, sulphosuccinimidyl 6-[3′-(2-pyridyldithio)-propionamido]hexanoate.

* To whom correspondence should be addressed.

lower virus dose. Although a number of strategies for coupling adenovirus with DNA–polycation complex have been proposed, all are dependent on infectious virions for efficient gene transfer [15,16]. This introduces the possibility of virus-mediated effects that compromise the stability of transgene expression *in vivo* [17,18]. Inactivation by psoralen before conjugation can substantially decrease, but not eliminate, the infectious titre of the virus [19]. Nevertheless, these results are important in providing direct evidence that the release of a DNA–polylysine complex from early endocytotic vesicles is a limiting factor to gene transfer, and suggest strategies for improved formulations.

Bacteria represent another class of pathogen that contain toxins that traverse vesicle membranes after receptor-mediated endocytosis. Diphtheria toxin (DT), a 535-residue polypeptide that is secreted from lysogenized *Corynebacterium diphtheriae*, accomplishes this by a translocation event [20]. The protein is organized into three functional domains as shown by crystallographic data: a catalytic toxic fragment at the N-terminus (C domain), followed by an α-helical transmembrane sequence (T domain), and a receptor-binding region at the C-terminus (R domain) [21,22]. When the toxin is taken up by receptor-mediated endocytosis and sequestered into endosomes, the low-pH environment of the vesicle triggers a conformational change in the T domain [23] which induces membrane insertion and the formation of ion-selective channels [24–28]. Recent work from Zhan *et al*. [29] showed that a recombinant peptide of the T domain of DT permeabilized large unilamellar vesicles under acidic conditions, releasing entrapped solutes.

In this study we coupled the α-helical T domain to a DNA–polylysine complex and evaluated the resulting conjugate for efficiency of gene transfer in cultured cells.

MATERIALS AND METHODS

Oligonucleotide-directed PCR mutagenesis

The T domain of DT encoded by the corynebacteriophage b *tox* structural gene was cloned by PCR (see Figure 1). Oligonucleotide primers were synthesized in accordance with the cDNA sequence [30] that flanks the T domain as determined by crystallographic data [21]. The 5′ end of the cDNA (DTtm) was generated with a sense-strand primer, 5′-AAT CTT GAT TGG GAT GTC ATA-3′, that aligned with positions 607–627 of the *tox* gene, and the anti-sense-strand primer, 3′-GA CAG TCA ACG TTG TGA CAA C-5′, aligned with positions 1184–1204. A single base change was incorporated into the anti-sense-strand primer to introduce a Trp-398 (TGG) to Cys-398 (TGC) substitution at the C-terminus of DTtm. This residue served as the reactive group for polylysine conjugation. The template for PCR was a cloned fragment of the *tox* gene encoding the B fragment of DT (DT301; American Type Culture Collection). PCR reaction conditions were as described [31]. The 600 bp PCR product was purified by agarose gel electroelution and subcloned as a blunt-ended cDNA into the *Stu*I site of the bacterial expression vector pMAL-c (New England Biolabs). This plasmid was designated pMAL-DTtm. A second recombinant plasmid, pMAL-L-DTtm, was constructed to introduce an eight amino acid linker (ISEFELGT) between the factor Xa cleavage site and the start of the DTtm sequence. The blunt-ended DTtm PCR fragment described above was subcloned into the *Sma*I site of pUC18 and subsequently retrieved by digestion with *Eco*RI and *Pst*I. The additional polylinker sequence that was acquired during this step served as linker coding sequence. The modified DTtm cDNA was cloned into the *Eco*RI and *Pst*I sites of pMAL-cRI (New England Biolabs). All constructs were initially characterized by endonuclease restriction digests and subsequently verified by sequence analysis.

Expression and purification of recombinant protein

Cultures of *Escherichia coli* strain DH5α transformed with parental or recombinant expression vectors were grown to a density of 2×10^8 cells/ml. Isopropyl β-D-thiogalactoside (IPTG; Boehringer Mannheim) was added to a final concentration of 0.3 M and the culture grown for an additional 1–2 h. For analytical work, cells from 0.5 ml of culture were harvested by centrifugation, suspended in 0.5 ml of SDS gel loading buffer and boiled for 5 min. Samples were resolved by SDS/PAGE and stained with Coomassie Blue. Preparative quantities of fusion protein were extracted and purified from 1 litre cultures of transformed cells induced with IPTG for 2 h. Cells were harvested by centrifugation, suspended in 50 ml of lysis buffer [10 mM sodium phosphate/30 mM NaCl/0.25% Tween-20/10 mM 2-mercaptoethanol/10 mM EDTA/10 mM EGTA (pH 7.0)] and lysed by sonication. Solid NaCl was added to 0.5 M and cell debris removed by centrifugation. The clarified extract (50 ml at 2.5 mg protein/ml) was applied to a 2.5 cm × 10 cm amylose column (New England Biolabs) equilibrated with column buffer [10 mM sodium phosphate/0.5 M NaCl/1 mM sodium azide/10 mM 2-mercaptoethanol/1 mM EGTA (pH 7.0)] at a flow rate of 1.0 ml/min. The column was washed with buffer until no detectable protein (A_{280}) was eluted from the resin. Bound material was released with 10 mM maltose in column buffer. Protein-containing fractions were combined and the elution buffer was changed to TBSE buffer [50 mM Tris/HCl (pH 7.0)/150 mM NaCl/5 mM EDTA] by flow dialysis and concentrated in a stirred-cell apparatus (Amicon). Disulphide bonds that formed were reduced by treatment with 5 mM dithiothreitol (DTT) at 37 °C for 1 h. The mixture was centrifuged at 20000 ***g*** for 30 min at 4 °C to remove insoluble material and applied to a 1.5 cm × 90 cm Sephacryl S-200 gel filtration column (Pharmacia) equilibrated with TBSE buffer. Peak fractions were analysed by SDS/PAGE and quantified by the method of Bradford [32].

Synthesis of poly-L-lysine conjugates

Purified recombinant proteins containing a C-terminal thiol (MBP–DTtm, MBP–L-DTtm, MBP and DTtm) (where MBP stands for maltose-binding protein) were conjugated with poly-L-lysine through the heterobifunctional cross-linker sulpho-succinimidyl 6-[3′-(2-pyridyldithio)-propionamido]hexanoate (sulpho-LC-SPDP; Pierce). A 10 mg/ml solution of poly-L-lysine (64.8 kDa; Sigma) was prepared in Hepes-buffered saline [HBS; 20 mM Hepes (pH 7.8)/150 mM NaCl]. Sulpho-LC-SPDP was added to a concentration of 0.5 mM and the reaction was incubated at room temperature with stirring for 30 min. Derivatized poly-L-lysine was resolved from excess sulpho-LC-SPDP by gel filtration over a Bio-Gel P6-DG column equilibrated with TBSE buffer. The conjugation reaction was initiated by mixing SPDP-derivatized poly-L-lysine with recombinant protein at a molar ratio of 1:4 respectively. The reaction was incubated under argon at room temperature for 20 h. Poly-L-lysine conjugates containing MBP domains (MBP–DTtm, MBP–L-DTtm and MBP) were separated from unincorporated poly-L-lysine by amylose-affinity chromatography. Recombinant DTtm conjugated to poly-L-lysine was purified by cation-exchange chromatography. Asialo-orosomucoid (ASOR)–polylysine conjugate was prepared by digestion with neuraminidase (Boehringer Mannheim) and chemically coupled to poly-L-lysine (65 kDa) with 1-ethyl-3-(3-dimethylaminopropyl)carbodi-imide (Pierce)

[33]. The binding capacity of purified conjugates with plasmid DNA or RNA as a substrate was determined by gel-shift analysis [34].

Transcription and translation *in vitro*

A luciferase cDNA [35] was subcloned into *Hin*dIII–*Sma*I sites located in the polylinker of plasmid pSP64 (Promega). The cloning strategy placed the 5′ end of the cDNA immediately downstream of an SP6 promoter. The recombinant plasmid (pSP.Luc) was linearized with a unique *Pvu*II site downstream of the 3′ end of the luciferase cDNA. Preparative run-off transcripts were generated with SP6 polymerase in accordance with conditions provided with a Riboprobe Gemini Core kit (Promega). Reactions were supplemented with $m^7G(5')ppp(5')G$ (Boehringer Mannheim), yielding capped transcripts. Completed reactions were treated with DNase RQ1 (Promega) to remove plasmid template, then extracted twice with phenol/chloroform/3-methylbutan-1-ol (50:48:2) and once with chloroform/3-methylbutan-1-ol (24:1), and RNA was precipitated with ethanol. Pellets were washed with 70 % (v/v) ethanol and suspended in RNase-free water. Transcripts were analysed for integrity by agarose gel electrophoresis and tested for production of functional enzyme by using nuclease-treated rabbit reticulocyte lysates (Promega). Translation *in vitro* was performed under conditions optimized by the manufacturer of the reticulocyte lysates. Terminated reactions were assayed for luciferase activity by using beetle luciferin (Promega) as substrate and quantified with a Lumat LB 9501/16 luminometer (Berthold).

Transfections

Binary complexes were prepared by suspending 2.0 μg of plasmid DNA or RNA in 100 μl of HBS and adding dropwise to 100 μl of HBS containing various amounts of poly-L-lysine conjugate. For RNA-based complexes, RNasin (Promega) was added to inhibit potential nuclease activity. The mixture was incubated at room temperature for 30 min and added directly to cells. Ternary complexes were generated by adding a second poly-L-lysine conjugate in 100 μl of HBS to a preformed binary complex, and incubating at room temperature for an additional 15 min.

Cells were seeded in 35 mm wells and allowed to reach 80–90 % confluency (10^6 cells). Seeding medium was replaced with 0.8 ml of medium supplemented with 2 % (v/v) fetal bovine serum (FBS). Complexes were added directly to the medium and evenly distributed; 4 h after transfection, 1.0 ml of medium supplemented with 16 % (v/v) FBS was added to each well. At selected time points, cells were washed once with PBS and harvested by adding 100 μl of lysis buffer [25 mM Tris/phosphate buffer (pH 7.8)/2 mM DTT/2 mM 1,2-diaminocyclohexane-*N*,*N*,*N*′,*N*′-tetra-acetic acid/10 % (v/v) glycerol/1 % (v/v) Triton X-100]. After a 10 min incubation at room temperature, the lysate was collected and cell debris was removed by centrifugation. The clarified extract was assayed for luciferase activity and total protein as described above. Transfections were performed in duplicate and standardized for total protein. Experiments were repeated several times with essentially identical results. The standard deviations were less than 1–2 % of the means for all conditions except very low total luciferase activity.

RESULTS AND DISCUSSION

T-domain fusion proteins of DT are soluble and efficiently conjugated with poly-L-lysine

The T domain from DT encodes a 19 kDa peptide that folds into a series of nine α-helices arranged into three layers [21]. A DNA fragment spanning this region (DTtm, 22 kDa) was isolated from the catalytic and receptor domains by PCR and cloned downstream of the *mal*E gene in plasmid pMAL-c as shown in Figure 1. The anti-sense-strand primer was designed to convert Trp-398 to Cys-398, thus providing a reactive thiol for conjugation. The recombinant sequence predicted a 65 kDa fusion protein composed of MBP (42 kDa) at the N-terminus and the T domain of DT (DTtm) at the C-terminus (Figure 1).

A pilot experiment was performed to determine the solubility and stability of MBP–DTtm. Small-scale cultures of IPTG-induced bacteria transformed with pMAL-c or pMAL-DTtm were lysed by sonication and the clarified cell extract was analysed by SDS/PAGE. The expected 51 kDa MBP–LacZα protein was evident in cells transformed with pMAL-c (Figure 2, lanes 3 and 4). This band was not detected in an extract from cells transformed with the recombinant plasmid pMAL-DTtm that contained an IPTG-inducible 65 kDa protein, which is the predicted molecular mass of an MBP–DTtm fusion protein (Figure 2, lanes 1 and 2). The intracellular concentration of MBP–LacZα and MBP–DTtm increased from 1 to 2 h after induction (Figure 2), indicating that MBP–DTtm was stable and could be retrieved as a soluble protein.

An extract was prepared from a 1 litre culture of bacteria transformed with pMAL-DTtm and applied to an amylose affinity column. After the resin had been washed extensively with buffer, a single protein peak was eluted from the column with 10 mM maltose. Analysis of the pooled fractions on an SDS/polyacrylamide gel under non-reducing conditions revealed two major bands (65 and 120 kDa), the smaller of which corresponded in size to the MBP–DTtm fusion protein (Figure 3A). Only the 65 kDa species was evident in the presence of reducing agents, suggesting that the 120 kDa protein was the result of disulphide bond formation between monomer-length molecules (Figure 3A). Purified MBP–DTtm was treated with DTT to increase the molar concentration of free thiol groups that would be available for polylysine conjugation. Gel filtration of the reaction product revealed two protein peaks, the first of which was eluted with the void volume and the second at an approximate molecular mass of 66 kDa. Analysis of the fractions by SDS/PAGE under non-reducing conditions indicated that more than 80 % of the dimer was converted to monomer-length peptides. The higher-molecular-mass material (peak 1) did not seem to be due to dimers that were not cleaved, because both peaks contained approximately equal ratios of dimer to monomer. An alternative explanation is that peak 1 consisted of MBP–DTtm aggregates. This is supported by several reports that have shown DT can oligomerize under certain conditions [23,36]. The material under peak 2 (i.e. monomeric MBP–DTtm) was combined and used for poly-L-lysine conjugation.

Several attempts to cleave the DTtm domain from MBP with factor Xa (see Figure 1C for strategy) proved to be unsuccessful (see below). We reasoned, however, that the MBP domain might not interfere with DTtm endosomolytic activity. Other studies have shown that the fusion of heterologous protein sequence to the T domain does not disrupt membrane insertion or the formation of ion channels [37]. The reduced MBP–DTtm fusion protein was mixed in a reaction vessel with SPDP-derivatized poly-L-lysine to initiate disulphide exchange and synthesis of conjugates. Conjugates were purified from unincorporated poly-L-lysine by amylose affinity chromatography through recognition of the retained MBP domain.

The efficiency of the reaction was determined by analysing a sample of reduced MBP–DTtm before and after conjugation with poly-L-lysine. In the absence of a reducing agent, MBP–DTtm migrated primarily as a 65 kDa monomer, with minor

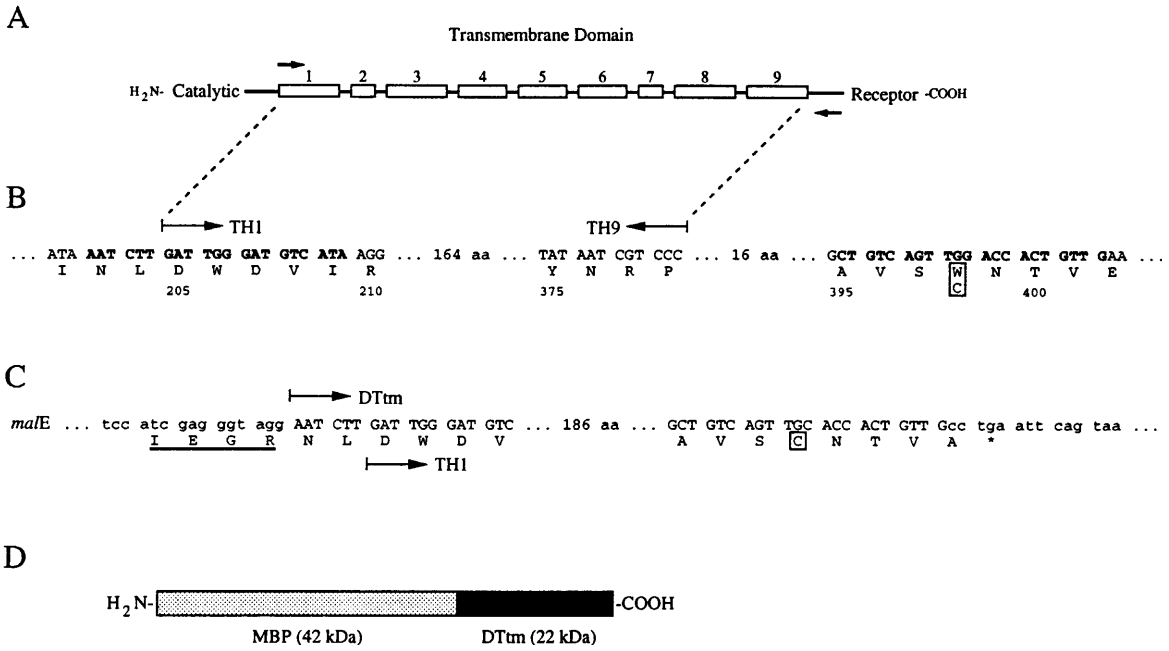

Figure 1 Cloning strategy for the T domain of DT

(**A**) The nine α-helices that comprise the T domain are shown flanked by the catalytic domain at the N-terminus and the receptor domain at the C-terminus. Sense-strand and anti-sense-strand PCR primers that were used to amplify the T domain are indicated by arrows. (**B**) Diagram of the nucleotide and amino acid sequences flanking the T domain of DT. Oligonucleotides for PCR were synthesized against the sequence shown in bold print. The Trp/Cys substitution shown at position 398 (boxed) was introduced by oligonucleotide-directed mutagenesis as described in the Materials and methods section. Arrows indicate the start of the first α-helix (TH1) and the end of the last α-helix (TH9) in the T domain. (**C**) Diagram of the partial nucleotide and amino acid sequence from recombinant plasmid pMAL-DTtm. The fusion site between the sequence downstream of the *mal*E gene and the N-terminus of the PCR cloned fragment DTtm is shown. The 5′ end of DTtm and the first α-helix (TH1) of the T domain are defined by arrows. The plasmid sequence is shown in lower case. The factor Xa cleavage site (IEGR) is underlined. A stop codon (marked with an asterisk) in the plasmid sequence occurs in-frame immediately 3′ of the C-terminus of the DTtm sequence. The cysteine residue used for polylysine conjugation is shown boxed. (**D**) Diagram showing the linear arrangement of the MBP–DTtm fusion protein. The MBP (42 kDa) is at the N-terminus and shaded; the cloned fragment of the toxin T domain (DTtm, 22 kDa) is represented as a solid box at the C-terminus.

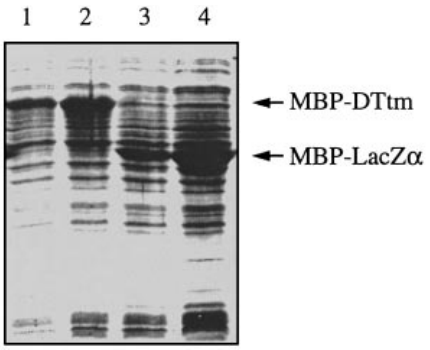

Figure 2 Bacterial expression of MBP–DTtm fusion protein

Cultures of *E. coli* strain DH5α transformed with recombinant plasmid pMAL-DTtm or the parent plasmid pMAL-c were induced with IPTG and harvested at selected time points. Extracts were prepared and resolved by SDS/PAGE [15% (w/v) gel] under reducing conditions. The gel was stained with Coomassie Blue. Lanes 1 and 2 contained cell extract from bacteria transformed with pMAL-DTtm at 1 and 2 h after induction respectively. Lanes 3 and 4 contained cell extract from bacteria transformed with pMAL-c at 1 and 2 h after induction respectively. The 65 kDa MBP–DTtm and 42 kDa MBP–LacZα fusion proteins are indicated.

contamination with dimer (Figure 4, lane 1). Under reducing conditions only the monomer band was evident (Figure 4, lane 3). A sample of MBP–DTtm after conjugation with poly-L-lysine and purification revealed a monomer band that was significantly lower in intensity (Figure 4, lane 2), even though an equivalent amount of protein was loaded on the gel (Figure 4; compare lanes 1 and 2). This diminished band represented MBP–DTtm that was not coupled to poly-L-lysine during synthesis. The large size and positive charge distribution of MBP–DTtm/poly-L-lysine conjugates prevented their migration into the resolving gel. Instead this material was found trapped in the stacking gel (results not shown). The MBP–DTtm moiety could be released from poly-L-lysine, however, by reducing the disulphide bond that linked the two components (Figure 4; compare lanes 2 and 4). More than 90% of reduced MBP–DTtm was conjugated with SPDP-derivatized poly-L-lysine, on the basis of the amount of monomer present in the resolving gel before and after reduction (Figure 4; compare lanes 2 and 4).

Gel-shift analysis indicated the charge contributed by 1 μg of plasmid DNA was completely neutralized by 5 μg of purified MBP–DTtm/poly-L-lysine (results not shown). Electron microscopy of binary complexes formulated at this ratio revealed distinct toroidal particles 50–100 nm in diameter (results not shown), similar to those described previously by Wagner et al. [2].

The T domain of DT increases the efficiency of DNA–polylysine complex gene transfer

A series of binary and ternary complexes were evaluated for gene transfer by using a luciferase expression vector (pCMVLuc). To study internalization by hepatic asialoglycoprotein receptors,

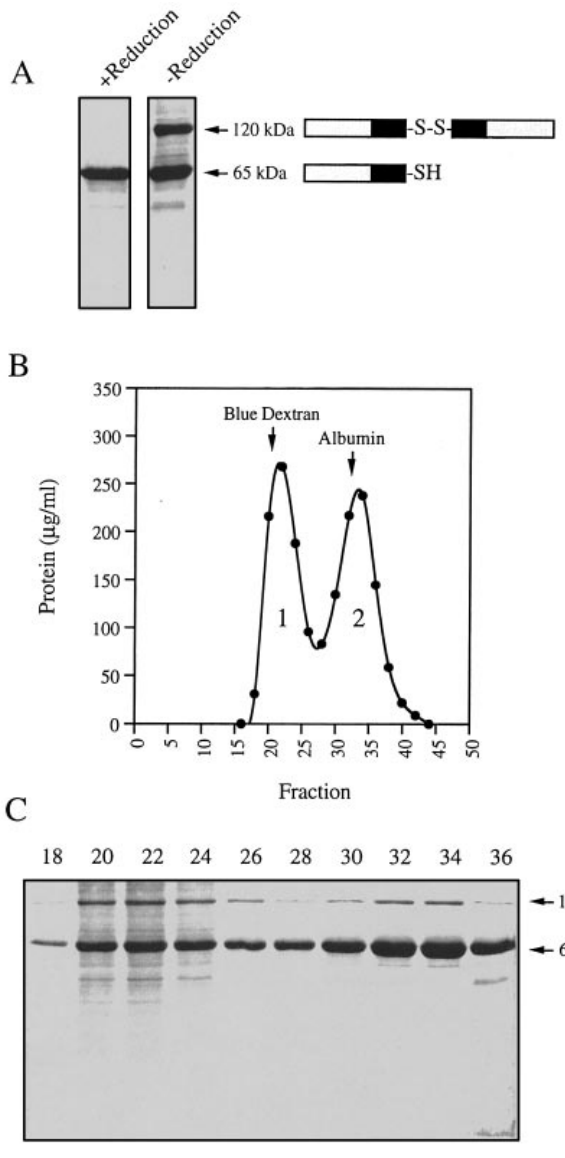

Figure 3 SDS/PAGE analysis of affinity-purified MBP–DTtm

(**A**) Clarified extract from IPTG-induced bacteria transformed with pMBP–DTtm was applied to an amylose affinity column. The column was extensively washed and bound material was eluted with 10 mM maltose. Peak fractions were combined and analysed by SDS/PAGE [12% (w/v) gel] in the presence (left-hand lane) or absence (right-hand lane) of reducing agent. Monomeric (65 kDa) and dimeric (120 kDa) forms of MBP–DTtm are indicated. (**B**) Affinity-purified MBP–DTtm was incubated with 5 mM DTT at 37 °C for 1 h, centrifuged at 20000 ***g*** for 30 min at 4 °C to remove insoluble material, and applied to a Sephacryl S-200 gel-filtration column. The elution profile is shown. Fractions (2.0 ml) were assayed for protein by the method of Bradford [32]. Protein concentration is shown on the ordinate, with the corresponding fraction numbers on the abscissa. Peaks 1 and 2 are labelled, as are the elution points of markers Blue Dextran (2 MDa) and BSA (66 kDa). (**C**) Alternating fractions through the two protein peaks (lanes labelled 18–36) were analysed by SDS/PAGE [12% (w/v) gel] in the absence of reducing agent. The 65 kDa monomeric and 120 kDa dimeric forms of MBP–DTtm are indicated. The gels in (**A**) and (**C**) were stained with Coomassie Blue.

binary complexes were formulated from pCMVLuc and an ASOR conjugate. Luciferase activity was approx. 10-fold higher in the asialoglycoprotein-expressing Huh7 cells transfected with the binary complex (Figure 5A, sample 3) than in cells that received plasmid alone (Figure 5A, sample 1). Consistent with previous studies, the level of expression was markedly enhanced

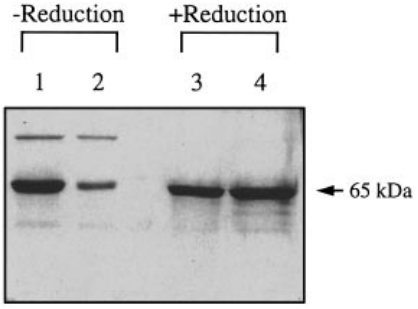

Figure 4 SDS/PAGE analysis of the fusion protein MBP–DTtm conjugated with polylysine

Reduced MBP–DTtm was coupled to SPDP-derivatized poly-L-lysine through the formation of a cleavable disulphide bridge. The conjugate was purified from unincorporated poly-L-lysine by amylose affinity chromatography and analysed by SDS/PAGE [12% (w/v) gel] in the absence (lane 2) or presence (lane 4) of reducing agent as indicated. A sample of the reduced MBP–DTtm fusion protein used for the conjugation reaction is also shown (lanes 1 and 2). Loaded samples (10 μg) were quantified relative to MBP–DTtm by the Bradford assay [32]. The gel was stained with Coomassie Blue.

by neutralizing intracellular acidic compartments with chloroquine (Figure 5A, sample 4) [16].

Complexes containing the MBP–DTtm conjugate were next tested for luciferase gene transfer. Cells transfected with a binary complex of pCMVLuc and MBP–DTtm conjugate revealed levels of luciferase expression that were relatively low (Figure 5A, sample 2), but significantly higher than plasmid alone (Figure 5A, sample 1). This suggested non-specific uptake of the complex by a mechanism other than endocytosis via the asialoglycoprotein receptor. Importantly, when these same binary complexes were provided with an ASOR ligand, thus forming a ternary complex, the level of gene transfer increased sharply (Figure 5A, samples 5–8). The highest level of luciferase expression occurred at a ternary ratio of 1:4:2 (plasmid/MBP–DTtm/ASOR), reflecting a 100-fold increase above that of the binary complex not containing DTtm (Figure 5A; compare samples 2 and 8). The efficiency of gene transfer with a ternary complex was influenced by changing the ratio of plasmid DNA to MBP–DTtm conjugate or ASOR conjugate (Figure 5A, samples 5–8). Another variable that was considered was the order in which each conjugate was added to plasmid DNA. Ternary complexes that were formulated in the reverse of the normal sequence (i.e. first mixing plasmid and ASOR conjugate, followed by the MBP–DTtm conjugate) were generally less efficient (Figure 5A, samples 9–12). This result might reflect differences in the exposure of ASOR or of MBP–DTtm, depending on the order of conjugate addition.

The specificity of vector internalization was tested with HL cells, a 3T3 clone that expresses a recombinant asialoglycoprotein receptor [38]. Parental 3T3 cells were used in this experiment as a negative control. Extracts from HL cells transfected with ASOR-containing binary complex in the presence of chloroquine showed 340-fold higher levels of luciferase activity than in similarly treated 3T3 cells (Figure 5B). The same trend was seen when cells were transfected with a ternary complex formulated in accordance with the optimal 1:4:2 ratio; gene transfer was 85-fold higher in HL cells.

Although the results in Figure 5 strongly suggested that the T domain facilitated gene transfer after receptor-mediated endocytosis, the presence of the MBP domain confounded this interpretation. Because we encountered difficulties in cleaving

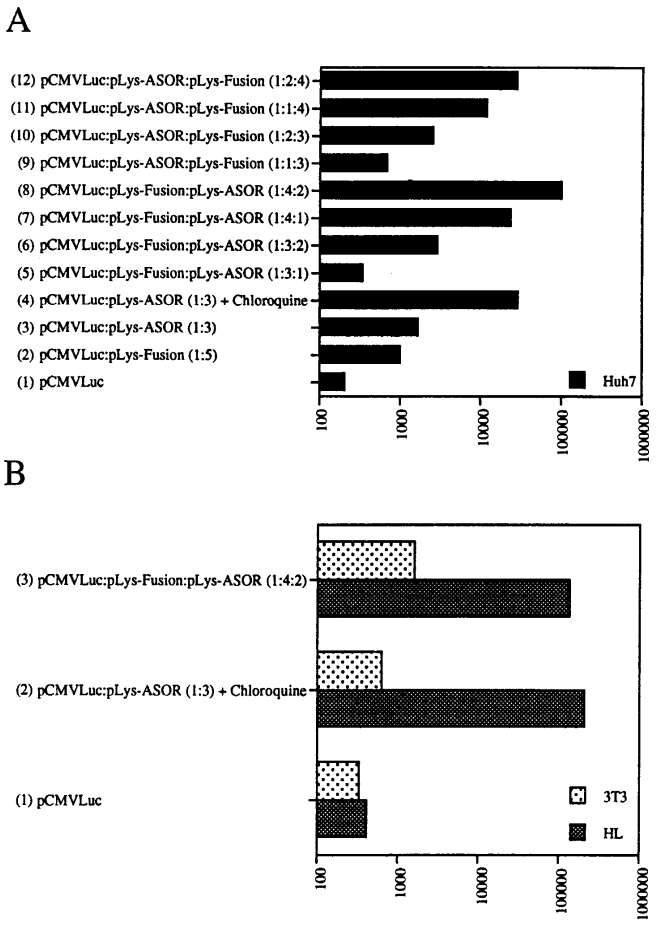

Figure 5 Luciferase expression in cells transfected with binary and ternary DNA–polylysine complex containing the fusion protein DTtm

Huh7 (**A**), 3T3 and HL (**B**) cells were seeded in 35 mm culture wells and grown to 80% confluency (10^6 cells per well). Seeding media were replaced with 0.8 ml media supplemented with 2% (v/v) FBS, before addition of transfection complex. Control wells (sample 1) received 2.0 μg of pCMVLuc suspended in 200 μl HBS. Binary complexes were assembled by adding pCMVLuc (2.0 μg) dropwise to poly-L-lysine conjugated with ASOR (pLys-ASOR) or MBP–DTtm (pLys-Fusion) and incubating the mixture at 23 °C for 30 min. For ternary complexes, a second conjugate in 100 μl of HBS was added to a preformed binary complex, followed by a 15 min incubation at 23 °C. The order in which conjugates were added is indicated by each ternary formulation. The ratio of each component in binary and ternary complexes is also given relative to a unit value of pCMVLuc (2.0 μg). Cells treated with chloroquine were incubated with the chemical at 50 μM during transfection. Cells were harvested 24 h after transfection, after which extracts were prepared and assayed for luciferase expression and total protein. Transfections were performed in duplicate. Binary and tertiary formulations are given on the ordinate. The abscissa shows luciferase expression in relative light units standardized to protein, and values are the means of total luciferase enzyme activity in 10^6 cells.

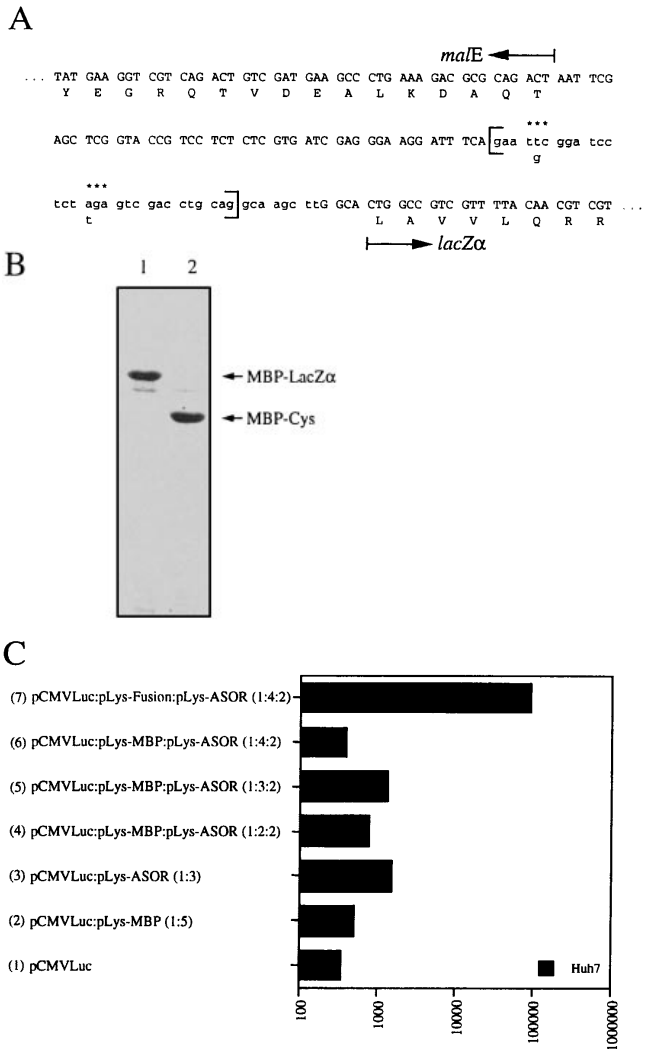

Figure 6 Evaluating the role of MBP in enhanced gene transfer

(**A**) The DNA sequence from the expression vector pMAL-cRI is shown that encodes the C-terminus of the MBP (labelled *mal*E) and the N-terminus of the β-galactosidase α peptide (labelled *lacZ*α). The multiple cloning site (lower-case lettering) between these two domains is also shown. An anti-sense-strand PCR primer was synthesized against the bracketed sequence in the multiple cloning site with the exception of two base changes as indicated. The alteration of T to G would cause a substitution of a Cys residue for Ser, thus providing a free thiol for conjugation with poly-L-lysine. The alteration of A to T would introduce a translation termination signal (TGA) to prevent read-through into the *lacZ*α sequence. PCR was performed with a sense-strand primer that mapped to the *mal*E gene 240 bp upstream of the anti-sense-strand primer (not shown). The PCR product containing the two point-mutations was subcloned into pMAL-cRI cassette, replacing the native sequence. The modified vector, pMAL-Cys, was transformed into DH5α. (**B**) Protein extracts from DH5α transformed with pMAL-cRI (lane 1) or pMAL-Cys (lane 2) were resolved by SDS/PAGE [12% (w/v) gel]. The migration of the 51 kDa MBP–LacZα fusion (MBP-LacZα) and the 42 kDa MBP containing a C-terminal cysteine residue (MBP-Cys) are shown. (**C**) DNA–protein complexes containing 2.0 μg of pCMVLuc and different combinations of poly-L-lysine conjugate were assembled and added to Huh7 cells (10^6) seeded in 35 mm culture wells. Poly-L-lysine conjugates of MBP–DTtm (pLys-Fusion), ASOR (pLys-ASOR) and MBP (pLys-MBP) were used to form binary (samples 2 and 3) and ternary (samples 4–7) complexes by using the guidelines described in Figure 5. Binary complexes containing pLys-MBP were formulated at a ratio of 1:5 (plasmid to conjugate) derived from gel-shift analysis (results not shown). Transfections were performed in duplicate. Formulations of complexes are given on the ordinate; the abscissa shows luciferase expression in relative light units standardized to total protein, and values are the means of total luciferase enzyme activity in 10^6 cells.

the DTtm peptide from the fusion protein early in the study, an alternative approach was devised to assess the involvement, if any, of the MBP domain. A modified MBP cDNA (MBP–Cys) that encoded a protein with a C-terminal cysteine residue was engineered as shown in Figure 6(A). A stop codon was introduced immediately 3′ of the cysteine residue to prevent read-through into the *lacZ*α gene. An extract from bacteria transformed with the plasmid carrying the modified MBP–Cys cDNA correctly expressed an IPTG-inducible protein that was approx. 10 kDa smaller than the native MBP–LacZα protein (Figure 6B). Preparative quantities of MBP–Cys were purified and used to synthesize a polylysine conjugate. When incorporated into a binary complex, the MBP conjugate had little effect on the efficiency of gene transfer beyond what could be achieved with plasmid alone (Figure 6C, samples 1 and 2). The addition of ASOR conjugate to the preformed binary complex resulted in a

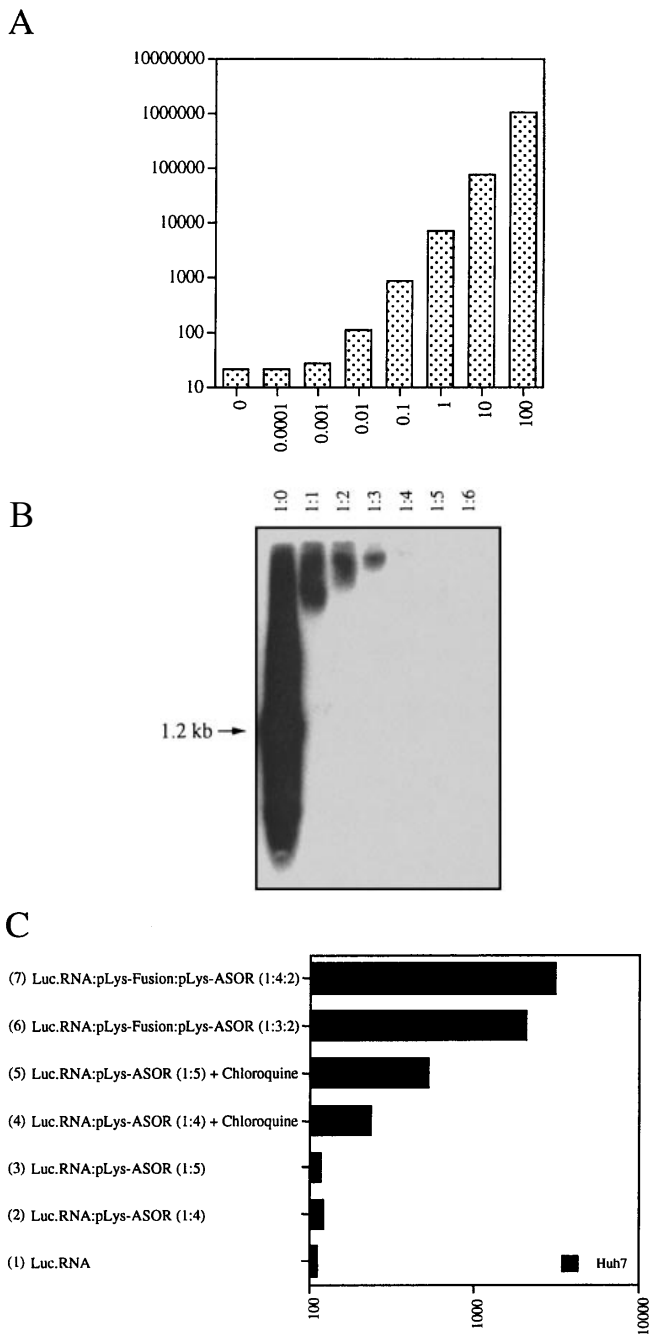

Figure 7 Luciferase expression in Huh7 cells transfected with an RNA–polylysine conjugate

(**A**) Increasing quantities of luciferase RNA transcribed *in vitro* was incubated with rabbit reticulocyte membranes and the products were assayed for enzyme activity. Luciferase expression in relative light units is given on the ordinate. The amount of luciferase RNA (in ng) that was added to the translation reaction *in vitro* is given along the abscissa. (**B**) RNA (100 ng) transcribed *in vitro* was incubated at 23 °C for 30 min with increasing amounts of poly-L-lysine conjugate (pLys-ASOR) and resolved on a 1.2% (w/v) agarose gel. The gel was electroblotted on a nylon membrane and hybridized with a random primer ^{32}P-labelled luciferase cDNA. As indicated along the top of the gel, the RNA-to-conjugate ratios that were tested ranged from 1:0 (100 ng of RNA to 0 ng of pLys-ASOR) to 1:6 (100 ng of RNA to 600 ng of pLys-ASOR). The position of migration of the 1.2 kb luciferase RNA transcript is indicated with an arrow. On shorter exposure to film, a distinct 1.2 kb band was evident. The apparent disappearance of transcript at higher ratios (e.g. 1:5 and 1:6) was due to the inability of RNA–polylysine complex to be electrophoretically transferred from the gel to the hybridization membrane. (**C**) Binary (samples 2–5) and ternary (samples 6 and 7) complexes containing 2.0 μg of luciferase RNA were assembled and added to Huh7 cells (10^6) seeded in 35 mm culture wells. Cells were harvested 9 h after transfection and assayed for luciferase activity. Transfections were performed in duplicate. Formulations of complexes are given on the ordinate; the abscissa shows luciferase expression in relative light units standardized to total protein, and values are the means of total luciferase enzyme activity in 10^6 cells.

minor increase in luciferase expression (Figure 6C, samples 4–6). However, these levels were no greater than a binary complex containing the ASOR conjugate alone (Figure 6C, sample 3). This finding was in sharp contrast to the substantial increase in luciferase expression that resulted when the ASOR conjugate was added to binary formulations that contained the MBP–DTtm fusion protein (Figure 6C, sample 7). These results suggest that the activity encoded by the MBP–DTtm fusion protein that increases the efficiency of gene transfer resides in the T domain of DT, not the MBP.

RNA transcripts can be delivered to the cytoplasm by ternary complex formulations

We were interested in determining whether the system described here could be adapted to deliver RNA to the cytoplasm of cells. Luciferase run-off transcripts were prepared and tested for production of functional enzyme. Translation *in vitro* with increasing amounts of luciferase RNA produced quantitative increases in enzyme activity (Figure 7A). The same transcript was evaluated for binding to an ASOR–polylysine conjugate by gel-shift analysis. The migration of the RNA transcript through an agarose gel was progressively retarded when preincubated with increasing amounts of conjugate (Figure 7B). At a ratio of 1:5 to 1:6 (RNA to conjugate; w/w), virtually all RNA was complexed with ASOR–polylysine. Electron microscopy of the RNA–polylysine complex formed at a 1:5 ratio revealed toroidal and rod-like structures that were similar in appearance to plasmid-based complexes, but less well defined (results not shown).

Binary complexes formulated with luciferase RNA and ASOR–polylysine at ratios of 1:4 and 1:5 were added to cultures of Huh7 cells and extracts were prepared 9 h after transfection. In the absence of an augmenting agent, neither formulation produced detectable levels of enzyme (Figure 7C, samples 2 and 3). However, when cells were treated with chloroquine, luciferase activity was detected in extracts from cells transfected with RNA complex prepared at a 1:5 ratio, and to a lesser extent at 1:4 (Figure 7C, samples 4 and 5). The efficiency of RNA delivery was increased further by incorporating the MBP–DTtm polylysine conjugate, thus forming a ternary complex. Here the levels of luciferase activity were 20–30-fold above background, depending on the formulation (Figure 7C, samples 6 and 7). These results suggest that RNA complexed with a polylysine conjugate can be transported to the cytoplasm and expressed in a manner that is dependent on endosomal release.

Gene transfer can be improved by removing the DTtm peptide from MBP

The inability to cleave recombinant fusion proteins proteolytically into their constituent parts is often attributed to local conformational folding that interferes with enzyme–substrate recognition [39]. We considered this possibility to explain the difficulties encountered in cleaving the transmembrane peptide from MBP–DTtm, where the recognition site for factor Xa construct was immediately adjacent to the first α-helix of the T domain (Figure 1C). A second fusion protein DNA was constructed that encoded a short peptide spacer between the

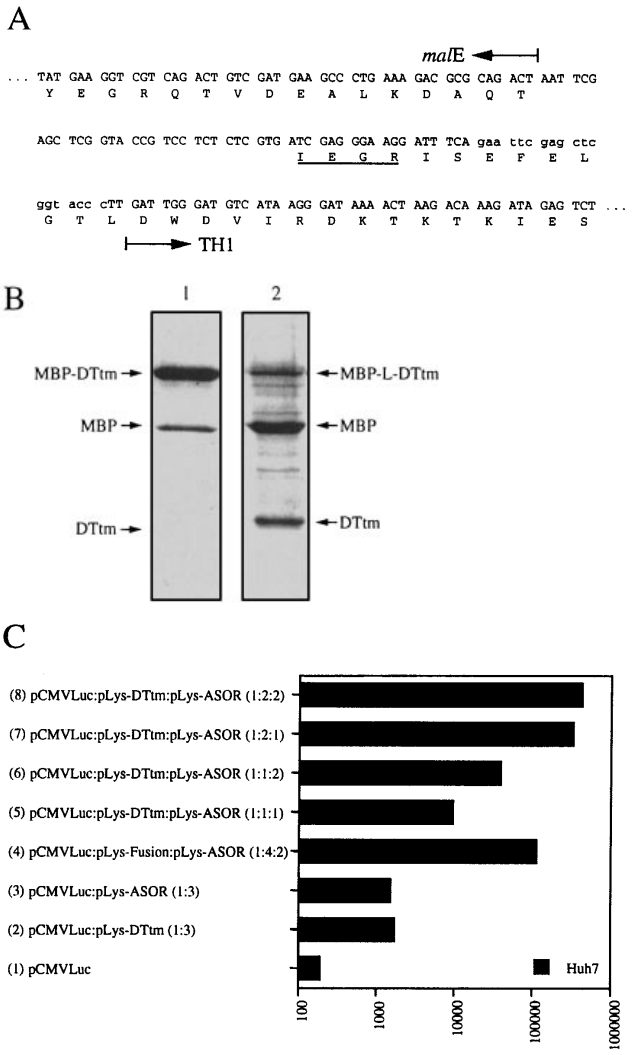

Figure 8 Transfection efficiency of DNA–polylysine complexes containing MBP-free DTtm conjugated to poly-L-lysine

(**A**) A sequence from the recombinant plasmid pMAL-LC-DTtm is shown that encodes the C-terminus of MBP (*malE*), factor Xa cleavage site (underlined) and the N-terminus of the first T domain α-helix (TH1). The polylinker sequence from plasmid pUC18 that was obtained during cloning is shown in lower-case lettering. The amino-acid linker sequence (ISEFELGTL) that was introduced to separate the factor Xa cleavage site from the first α-helix TH1 encoded by DTtm is also shown. (**B**) Affinity-purified samples of MBP–DTtm (lane 1) or MBP–LC-DTtm (lane 2) were digested with factor Xa and resolved by SDS/PAGE [12% (w/v) gel]. The gel was stained with Coomassie Blue. The migration of the 65 kDa fusion proteins (MBP-DTtm and MBP-L-DTtm), 42 kDa MBP and the 22 kDa T domain of DT (DTtm) are indicated. The molecular mass of DTtm in lane 2 is slightly higher than in lane 1 because of the linker sequence. (**C**) Huh7 cells (10^6) seeded in 35 mm culture wells were transfected with DNA–polylysine complex containing 2.0 μg of pCMVLuc and harvested 24 h later. Control cells (sample 1) received 2.0 μg of pCMVLuc in 200 μl of HBS. Extracts were prepared and analysed for luciferase activity and protein. The formulations for binary (samples 2 and 3) and ternary (samples 4–8) complexes are given on the ordinate; the abscissa shows luciferase expression in relative light units standardized to total protein, and values are the means of total luciferase enzyme activity in 10^6 cells.

factor Xa cleavage site and the start of the DTtm peptide (Figure 8A). In addition to the linker sequence, a mild denaturation step (1 M guanidine hydrochloride) was introduced to facilitate enzyme–substrate recognition. This combination markedly enhanced site-specific proteolytic cleavage of affinity-purified MBP–L-DTtm into MBP and DTtm. More than 90% of the fusion protein was correctly processed, compared with less than 10% of the original MBP–DTtm fusion protein (Figure 8B).

The DTtm peptide was separated from MBP and undigested MBP–L-DTtm by amylose-affinity chromatography; free DTtm was eluted from the column as a single peak during the binding step. A DTtm–polylysine conjugate was prepared and found to condense plasmid DNA fully at a ratio of 1:3 (plasmid to conjugate) according to gel-shift analysis and electron microscopy (results not shown). Binary complexes containing the DTtm peptide displayed non-specific gene transfer to Huh7 cells in a manner similar to the intact fusion protein (Figure 8C, sample 2). However, with the addition of an ASOR ligand, gene transfer and luciferase expression reached a maximum level that was 250-fold that generated with the binary complex (Figure 8C; compare samples 2 and 8). The efficiency of transfection in a ternary complex increased in proportion to the amount of DTtm (Figure 8C, samples 5–8). A comparison of luciferase expression in cells transfected with ternary complex containing the intact MBP–DTtm fusion protein or the isolated DTtm peptide indicated that a 4-fold improvement in gene transfer was obtained by removing the MBP domain from DTtm (Figure 8C; compare samples 4 and 8).

During the course of the preceding experiments, close attention was paid to the toxicity of conjugates that contained either the MBP–DTtm fusion protein or the DTtm peptide. Although we noted a slight degree of cell rounding and detachment at the end of the 24 h incubation period, this response was independent of the formulation. For instance, cells that were exposed to ternary complex containing a mixture of 4 μg of pLys–DTtm and 4 μg of pLys–ASOR (Figure 8, sample 8) were identical in appearance with cells transfected with binary complex containing either 6 μg of pLys–ASOR (Figure 8, sample 3) or 6 μg of pLys–DTtm (Figure 8, sample 2). Furthermore, cells treated with the different complex formulations continued to grow normally and expanded to a confluent monolayer after 24 h. These observations suggest that the endosomolytic activity of DTtm can be achieved without introducing toxic side effects.

In our cell culture model, each of the experiments was designed to evaluate gene transfer levels at relatively early time points (i.e. 24 h). Although the data provided insight into the efficiency of gene transfer, we did not determine whether our protocol extended the persistence of the delivered plasmid vector. Other groups have reported that DNA–protein complex formulations with improved delivery efficiency also display prolonged gene expression when the vehicle is tested *in vivo* [7]. To what extent transfection particles containing the DTtm peptide improve vector persistence *in vivo* will be investigated in a future study.

There are many examples in nature of membrane disruption induced by components of viruses and other pathogens that use receptor-mediated endocytosis as a route to cell entry [40]. These biological processes have been exploited in strategies to improve the efficiency of synthetic, ligand-tagged vectors. In this study we evaluated the utility of the T domain of DT for conferring endosomolytic activity on molecular conjugates because of its demonstrated propensity for inserting into membranes at low pH. This domain has been extensively studied by crystallographic imaging and mutational analysis, revealing important structure–function relationships [20].

The T domain of DT encodes a series of nine α-helices arranged into three layers [21,22]. The innermost layer contains two hydrophobic helices, TH8 (21 residues) and TH9 (23 residues), joined by an acidic loop (TL5). Helices TH5–TH7 are similarly apolar and form an intermediate layer that wraps around the TH8–TH9 hairpin. The third and outermost layer of helices, TH1–TH4, is positively charged at low pH and probably

serves as the initial contact face with phospholipid headgroups of the membrane. When exposed to acidic pH (approx. 5.0), the T domain undergoes local conformational changes that enable the three layers to separate. Critical to subsequent membrane insertion is the partial protonation of the acidic loop (TL5) that connects hydrophobic helices TH8 and TH9. The increased membrane-solubility of TL5 facilitates its interaction with the membrane surface, thereby driving the two connecting apolar helices into the endosome bilayer. On exposure to the neutral cytosolic face (pH approx. 7.5), the acidic residues in TL5 should reionize, stabilizing the transmembrane configuration of the TH8–TH9 hairpin. On this model, the layers defined by helices TH1–TH4 and TH5–TH7 remain at the luminal surface of the endosome [21,41].

In addition to the central role that TH8–TH9 plays in securing the T domain to the endosome membrane, this hydrophobic hairpin is believed to mediate membrane depolarization by forming an ion channel [37,41]. Experiments with isolated vesicles, artificial membranes and whole cells indicate that the pore is a single channel specific for monovalent cations, with some differences in the channel conductance depending on the model system [27,28,42–45]. Despite the apparent correlation between membrane depolarization and translocation of the catalytic A fragment, the precise relationship between the two events remains unclear. It has been proposed that toxin-induced pores might serve as a protein 'tunnel' through which the extended A fragment passes [28,46]; however, there is no direct evidence to support this model. A less precise translocation mechanism that has been considered involves pore formation that is sufficiently large (i.e. diameter and frequency) to cause severe distortions in the lipid bilayer, culminating in bulk release of luminal contents [20,43]. This latter model resembles the disruptive action of haemolytic agents, including *Staphylococcus aureus* a toxin and components of activated complement [40]. In much the same manner, pores formed by DT have been associated with the pH-dependent leakage of small (calcein) and large (70 kDa dextran) molecules from unilamellar vesicles [43]. Importantly, the isolated T domain is nearly equivalent to the holotoxin in its ability to induce membrane depolarization and permeability at low pH [29,37,41].

In the present study, recombinant T domain expressed in *E. coli* markedly improved the efficiency of gene transfer when coupled to a DNA–polylysine carrier complex. The effect could be achieved when the T domain was presented as an MBP fusion protein or as an independent peptide. Considering the activities that have been assigned to the T domain, it is difficult to imagine that the ion channel formed by the TH8–TH9 hairpin can act as a gate for a large DNA–polycation complex (100 nm or more), particularly if the reported pore diameter of 1.8–2.2 nm is accurate [26,28,46]. This is not to suggest, however, that the induction of an ion flux across the endosome membrane might not be relevant. It is possible that the influx of H^+ and Na^+ ions through the channel, accompanied by an efflux of K^+ ions, could decrease the membrane potential, collapse the pH gradient and ultimately destabilize vesicle integrity. This process would probably be amplified in the context of a DNA–polylysine complex that displayed clustered T domains. Indeed, several reports have shown that the extent of pore formation, and therefore membrane permeability, is proportional to the concentration of toxin at the membrane surface [20]. A potential contributing factor to this is the ability of DT to oligomerize in solution, and possibly on membranes as well [23,36]. This behaviour has significance for the present study because we observed a similar aggregation of the MBP–DTtm fusion protein (Figure 3). Although the relevance of oligomerization to enhanced gene transfer remains uncertain, the positive co-operativity of the T domain seemed to be evident in our model system based on the dose response that was observed (Figures 5 and 8).

The results presented here mirror earlier studies that used α-helical peptides derived from the N-terminus of influenza virus haemagglutinin HA-2 to enhance the delivery of endocytosed DNA–polylysine complex [47]. Synthetic, amphipathic peptides designed to assume an α-helical conformation at low pH have also been shown to facilitate gene transfer [48]. In general these endosomolytic peptides share at least two properties, namely pH-dependent leakage of membrane-entrapped solutes (e.g. fluorophores) and a positive dose response for membrane permeability and gene transfer. Zhan et al. [29] recently showed that a recombinant form of the T domain expressed in *E. coli* was capable of disrupting unilamellar vesicles under acidic conditions. In those experiments the rate of fluorophore release was found to be rapid, with a linear dependence on T domain concentration. Those results, together with our finding that the isolated T domain can induce the release of endocytosed DNA–polylysine complex, suggest a mechanism that is similar to endosomolytic peptides. Future studies will be important to characterize further the membrane-disrupting properties of the T domain from DT, and to determine the minimal sequence requirements. Work by Silverman et al. [37] suggests that a short 61-residue stretch that corresponds to the TH8–TH9 hairpin shows single-channel conductance and ion selectivity nearly identical with that of the intact T domain. Whether this truncated domain maintains endosomolytic activity is being investigated.

This work was supported by grants from the NIDDK of the NIH, the Cystic Fibrosis Foundation, and Genovo, a company of which J.M.W. is a founder and in which he holds equity.

REFERENCES

1 Wu, G. Y. and Wu, C. H. (1987) J. Biol. Chem. **262**, 4429–4432
2 Wagner, E., Zenke, M., Cotten, M., Beug, H. and Birnstiel, M. L. (1990) Proc. Natl. Acad. Sci. U.S.A. **87**, 3410–3414
3 Ferkol, T., Perales, J. C., Eckman, E., Kaetzel, C. S., Hanson, R. W. and Davis, P. B. (1995) J. Clin. Invest. **95**, 493–502
4 Olins, D. E., Olins, A. L. and Von Hippel, P. H. (1967) J. Mol. Biol. **24**, 157–162
5 Cohen, P. and Kidson, C. (1968) J. Mol. Biol. **35**, 241–245
6 Carroll, D. (1972) Biochemistry **11**, 421–426
7 Perales, J. C., Ferkol, T., Beegen, H., Ratnoff, O. D. and Hanson, R. W. (1994) Proc. Natl. Acad. Sci. U.S.A. **91**, 4086–4090
8 Chowdhury, N. R., Wu, C. H., Wu, G. Y., Yerneni, P. C., Bommineni, V. R. and Chowdhury, J. R. (1993) J. Biol. Chem. **268**, 11265–11271
9 Gerber, U. F., Willetts, M., Webster, P. and Helenius, A. (1993) Cell **75**, 477–486
10 Seth, P., Pastan, I. and Willingham, M. C. (1985) J. Biol. Chem. **260**, 9598–9602
11 Yoshimura, A. (1985) Cell Struct. Funct. **10**, 391–404
12 Defer, C., Belin, M.-T., Caillet-Boudin, M.-L. and Boulanger, P. (1990) J. Virol. **64**, 3661–3673
13 Curiel, D. T., Agarwal, S., Wagner, E. and Cotten, M. (1991) Proc. Natl. Acad. Sci. U.S.A. **88**, 8850–8854
14 Curiel, D. T., Wagner, E., Cotten, M., Birnstiel, M. L., Agarwal, S., Li, C.-M., Loechel, S. and Hu, P.-C. (1992) Human Gene Therapy **3**, 147–154
15 Wagner, E., Zatloukal, K., Cotten, M., Kirlappos, H., Mechtler, K., Curiel, D. T. and Birnstiel, M. L. (1992) Proc. Natl. Acad. Sci. U.S.A. **89**, 6099–6103
16 Fisher, K. J. and Wilson, J. M. (1994) Biochem. J. **299**, 49–58
17 Yang, Y., Ertl, H. C. J. and Wilson, J. M. (1994) Immunity **1**, 433–442
18 Yang, Y., Li, Q., Ertl, H. C. J. and Wilson, J. M. (1995) J. Virol. **69**, 2004–2015
19 Cotten, M., Wagner, E., Zatloukal, K., Phillips, S., Curiel, D. T. and Birnstiel, M. L. (1992) Proc. Natl. Acad. Sci. U.S.A. **89**, 6094–6098
20 London, E. (1992) Biochim. Biophys. Acta **1113**, 25–51
21 Choe, S., Bennett, M. J., Fujii, G., Curmi, P. M. G., Kantardjieff, K. A., Collier, R. J. and Eisenberg, D. (1992) Nature (London) **357**, 216–222
22 Bennett, M. J. and Eisenberg, D. (1994) Protein Science **3**, 1464–1475
23 Blewitt, M. G., Chung, L. A. and London, E. (1985) Biochemistry **24**, 5458–5464
24 Sandvig, K. and Olsnes, S. (1981) J. Biol. Chem. **256**, 9068–9076
25 Hu, V. and Holmes, R. K. (1984) J. Biol. Chem. **259**, 12226–12233

26 Zalman, L. S. and Wisnieski, B. I. (1984) Proc. Natl. Acad. Sci. U.S.A. **81**, 3341–3345
27 Donovan, J. J., Simon, M. I., Draper, R. K. and Montal, M. (1981) Proc. Natl. Acad. Sci. U.S.A. **78**, 172–176
28 Kagan, B. L., Finkelstein, A. and Colombini, M. (1981) Proc. Natl. Acad. Sci. U.S.A. **78**, 4950–4954
29 Zhan, H., Oh, K. J., Shin, Y.-K., Hubbell, W. L. and Collier, R. J. (1995) Biochemistry **34**, 4856–4863
30 Greenfield, L., Bjorn, M. J., Horn, G., Fong, D., Buck, G. A., Collier, R. J. and Kaplan, D. A. (1983) Proc. Natl. Acad. Sci. U.S.A. **80**, 6853–6857
31 Fisher, K. J. and Aronson, Jr., N. N. (1991) J. Biol. Chem. **266**, 12105–12113
32 Bradford, M. (1976) Anal. Biochem. **72**, 248–252
33 Wilson, J. M., Grossman, M., Wu, C. H., Chowdhury, N. R., Wu, G. Y. and Chowdhury, J. R. (1992) J. Biol. Chem. **267**, 963–967
34 Wu, G. Y. and Wu, C. H. (1988) Biochemistry **27**, 887–892
35 De Wet, J. R., Wood, K. V., DeLuca, M., Helinski, D. R. and Subramani, S. (1987) Mol. Cell. Biol. **7**, 725–737
36 Papini, E., Schiavo, G., Tomasi, M., Colomatti, M., Rappuoli, R. and Montecucco, C. (1987) Eur. J. Biochem. **169**, 637–644
37 Silverman, J. A., Mindell, J. A., Zhan, H., Finkelstein, A. and Collier, R. J. (1994) J. Membrane Biol. **137**, 17–28
38 Bunnell, B., Askari, F. and Wilson, J. (1992) Somat. Cell Mol. Gen. **18**, 559–569
39 Nagia, K. and Thogersen, H. C. (1987) Methods Enzymol. **153**, 461–481
40 Bashford, C. L., Alder, G. M., Menestrina, G., Micklem, K. J., Murphy, J. J. and Pasternak, C. A. (1986) J. Biol. Chem. **261**, 9300–9308
41 Zhan, H., Choe, S., Huynh, P. D., Finkelstein, A., Eisenberg, D. and Collier, R. J. (1994) Biochemistry **33**, 11254–11263
42 Shiver, J. W. and Donovan, J. J. (1987) Biochim. Biophys. Acta **903**, 48–55
43 Jiang, G.-S., Solow, R. and Hu, V. W. (1989) J. Biol. Chem. **264**, 13424–13429
44 Papini, E., Sandona, D., Rappuoli, R. and Montecucco, C. (1988) EMBO J. **11**, 3353–3359
45 Eriksen, S., Olsnes, S., Sandvig, K. and Sand, O. (1994) EMBO J. **13**, 4433–4439
46 Hoch, D. H., Romero-Mira, M., Ehrlich, B., Finkelstein, A., DasGupta, B. R. and Simpson, L. L. (1985) Proc. Natl. Acad. Sci. U.S.A. **82**, 1692–1696
47 Wagner, E., Plank, C., Zatloukal, K., Cotten, M. and Birnstiel, M. L. (1992) Proc. Natl. Acad. Sci. U.S.A. **89**, 7934–7938
48 Plank, C., Oberhauser, B., Mechtler, K., Koch, C. and Wagner, E. (1994) J. Biol. Chem. **269**, 12918–12924

Received 17 April 1996/16 August 1996; accepted 27 August 1996